The Influence of the CTIP Polymorphism, Q418P, on Homologous Recombination and Predisposition to Radiation-Induced Tumorigenesis (mainly rAML) in Mice

Authors: Patel, Agata, Anderson, Jennifer, Kraft, Daniela, Finnon, Rosemary, Finnon, Paul, et al.

Source: Radiation Research, 186(6) : 638-649

Published By: Radiation Research Society

URL: https://doi.org/10.1667/RR14495.1

RADIATION RESEARCH **186**, 638–649 (2016)
0033-7587/16 $15.00

DOI: 10.1667/RR14495.1

The Influence of the CTIP Polymorphism, Q418P, on Homologous Recombination and Predisposition to Radiation-Induced Tumorigenesis (mainly rAML) in Mice

Agata Patel,[a,b,1] Jennifer Anderson,[b] Daniela Kraft,[c] Rosemary Finnon,[a] Paul Finnon,[a] Cheryl L. Scudamore,[d] Grainne Manning,[a] Robert Bulman,[a] Natalie Brown,[a] Simon Bouffler,[a] Peter O'Neill[b] and Christophe Badie[a]

[a] *Cancer Genetics and Cytogenetics Group, Radiation Effects Department, Centre for Radiation Chemical and Environmental Hazards, Public Health England, Chilton, Didcot, Oxfordshire, OX11 0RQ, United Kingdom;* [b] *DNA Damage Group, Oxford Institute for Radiation Oncology, University of Oxford, Oxford, OX3 7DQ, United Kingdom;* [c] *GSI Helmholtzzentrum für Schwerionenforschung GmbH Planckstraße 1, 64291 Darmstadt, 11-05-52, Germany; and* [d] *Mary Lyon Centre, MRC Harwell, Harwell Science and Innovation Campus, Oxfordshire, OX11 0RD, United Kingdom*

Patel, A., Anderson, J., Kraft, D., Finnon, R., Finnon, P., Scudamore, C. L., Manning, G., Bulman, R., Brown, N., Bouffler, S., O'Neill, P. and Badie, C. The Influence of the CTIP Polymorphism, Q418P, on Homologous Recombination and Predisposition to Radiation-Induced Tumorigenesis (mainly rAML) in Mice. *Radiat. Res.* 186, 638–649 (2016).

Exposure to ionizing radiation increases the incidence of acute myeloid leukemia (AML), which has been diagnosed in Japanese atomic bombing survivors, as well as patients treated with radiotherapy. The genetic basis for susceptibility to radiation-induced AML is not well characterized. We previously identified a candidate murine gene for susceptibility to radiation-induced AML (rAML): C-terminal binding protein (CTBP)-interacting protein (CTIP)/retinoblastoma binding protein 8 (RBBP8). This gene is essential for embryonic development, double-strand break (DSB) resection in homologous recombination (HR) and tumor suppression. In the 129S2/SvHsd mouse strain, a nonsynonymous single nucleotide polymorphism (nsSNP) in *Ctip*, Q418P, has been identified. We investigated the role of Q418P in radiation-induced carcinogenesis and its effect on CTIP function in HR. After whole-body exposure to 3 Gy of X rays, 11 out of 113 (9.7%) 129S2/SvHsd mice developed rAML. Furthermore, 129S2/SvHsd mouse embryonic fibroblasts (MEFs) showed lower levels of recruitment of HR factors, Rad51 and replication protein A (RPA) to radiation-induced foci, compared to CBA/H and C57BL/6 MEFs, isolated from rAML-sensitive and resistant strains, respectively. Mitomycin C and alpha particles induced lower levels of sister chromatid exchanges in 129S2/SvHsd cells compared to CBA/H and C57BL/6. Our data demonstrate that Q418P nsSNP influences the efficiency of CTIP function in HR repair of DNA DSBs *in vitro* and *in vivo*, and appears to affect susceptibility to rAML. © 2016 by Radiation Research Society

Editor's note. The online version of this article (DOI: 10.1667/RR14495.1) contains supplementary information that is available to all authorized users.

[1] Address for correspondence: Oxford Institute for Radiation Oncology, Old Road Campus Research Building, Oxford, OX3 7DQ, United Kingdom; email: agata.patel@oncology.ox.ac.uk.

INTRODUCTION

Genetic mutations can be acquired or inherited through the germline. Although cancer is most commonly associated with acquired mutations, the identification of inheritable cancer predisposition genes is of great importance as well. Over the last 30 years, more than 100 cancer predisposition genes have been discovered (*1*). In genome-wide association studies (GWAS) of hundreds of thousands of single nucleotide polymorphisms (SNPs), susceptibility loci in cancer predisposition genes have been identified for several solid tumors (*2, 3*), chronic lymphocytic leukemia (*4*), acute lymphoblastic leukemia (*5*) and acute myeloid leukemia (AML) (*6*).

Exposure to ionizing radiation increases the mutation rate and risk of cancer, including AML. Although therapy-related AML (t-AML) is an important late adverse effect of radiation and chemotherapy, to date, few genetic variants that confer susceptibility to t-AML have been detected. We previously identified the C-terminal binding protein (CTBP)/interacting protein (CTIP)/retinoblastoma binding protein 8 (RBBP8) gene, located on mouse chromosome 18, as potentially associated with rAML (*7*). CTIP is a large nuclear protein conserved among vertebrates and a cofactor for the transcriptional corepressor CTBP (*8*). CTIP also interacts with tumor suppressors such as BRCA1 (*9*) and the retinoblastoma protein (RB) family members through binding sites that are frequently mutated in human cancers (*10*). CTIP is a target for BRCA1-dependent phosphorylation by ataxia telangiectasia mutated (ATM) kinase, which is induced by DNA double-strand breaks (DSBs) (*11*). It is required for DNA DSB resection, particularly in homologous recombination (HR) (*12*) but also in single-strand annealing (SSA) and alternative non-homologous end-joining (alt-NHEJ) for minor resection of broken ends (*13*). Homozygous inactivation of the *Ctip* gene causes very early embryonic lethality during mouse development and *Ctip* heterozygous mice develop tumors, principally lym-

phomas, suggesting that CTIP functions as a tumor suppressor (*14*).

Upon DNA damage induction, CTIP binds to the MRE11, Rad50 and NBS1 (MRN) complex, prior to its phosphorylation by ataxia telangiectasia and Rad3-related (ATR) protein (*15*), CDK2 and ATM, as well as its ubiquitination by BRCA1 (*16*). CTIP with the MRN complex initiates DSB resection by endonucleolytic cleavage of 5′ DNA termini. The resection is continued by endonucleases EXO1 and DNA2 with the help of bloom syndrome helicase (BLM). The ssDNA is subsequently bound by replication protein A (RPA), which is then replaced by RAD51 to form a ssDNA-RAD51 nucleofilament. RPA, mainly activated by DNA-PKcs after DNA damage, can recruit ATR, which in response phosphorylates CHK1 to promote G_2/M- or intra-S-phase checkpoint activation (*17*).

Since CTIP is a crucial protein for embryonic development, DNA repair and cell cycle progression, impairment of its functions could cause severe phenotypes. In this study, we identified an inbred mouse strain carrying a Q418P nsSNP in *Ctip*, which was predicted to be disease-causing by several algorithms. This nsSNP impairs the HR repair of DSBs, after gamma and alpha irradiation, as well as hydroxyurea (HU) or mitomycin C (MMC) treatment. This in turn contributes to an increased complexity of radiation-induced chromosomal aberrations and is likely to play a role in increasing risk of radiation-induced carcinogenesis, specifically rAML.

MATERIALS AND METHODS

The details for CTIP knockdown and overexpression, DNA and RNA extraction, PCR, RT-PCR, immunofluorescence, sister chromatid exchanges (SCEs), Western blot, aCGH, FACS, clonogenic assay and statistics are described in the Supplementary Material and Methods (http://dx.doi.org/10.1667/RR14495.1.S1).

In Vivo Studies

The CBA/H mouse strain was obtained from the Medical Research Council (Harwell, UK), and the C57BL/6JOlaHsd and 129S2/SvHsd mouse strains were obtained from Harlan SeraLab (Loughborough, UK). The *in vivo* work performed here was granted appropriate licensing from the UK Home Office under the regulation of the Animals (Scientific Procedures) Act 1986 (ASPA) and with approval of the PHE CRCE Animal Welfare and Ethical Review Body (AWERB). At 12–15 weeks of age, mice were whole-body exposed to 3 Gy of X rays, the optimal dose for AML induction in the CBA/H strain (*18*), at a dose rate 0.7 Gy min^{-1} using an AGO HS X-ray system (250 kV,14 mA; Sheffield, UK) and were monitored daily postirradiation for signs of lethargy, poor grooming, hunched posture and rapid breathing. Any mouse showing any three of these signs was euthanized with a rising concentration of CO_2. Postmortem blood samples were taken from the hearts of suspected AML cases as well as controls and used to assess indicators of AML: neutropenia, splenomegaly, elevated total white blood cell count and presence of leukemic blasts (*41*).

Mouse Embryonic Fibroblasts

Mouse embryonic fibroblasts (MEFs) were isolated from CBA/H, C57BL/6 and 129S2/SvHsd mice on day 13 of pregnancy, and cultured in DMEM with GlutaMAX™ (Invitrogen Inc., Paisley, UK) growth media supplemented with 10% fetal bovine serum (FBS; Life Technologies, Carlsbad, CA) and penicillin/streptomycin (Sigma-Aldrich Inc., Poole, Dorset, UK) at standard concentrations (Invitrogen). Primary MEFs were maintained at 3% oxygen (5% CO_2, 37°C) to allow better growth.

Mouse embryonic fibroblasts were immortalized either by knockdown of p53 protein, using a pRS(Puro)-p53shRNA (used only for the transfection with the Rbbp8-pCMV6 plasmid for CTIP overexpression), or by SV40 immortalization, using the pZip-LT plasmid (used for all experiments in this study apart from CTIP overexpression).

Immortalized MEFs were cultured at 21% O_2 (5% CO_2, 37°C). Primary and immortalized cell lines were subcultured to maintain log-phase growth.

Bioinformatics

A benchmark dataset containing over 43,000 SNPs was employed for the unbiased evaluation of eight established prediction tools: MAPP; PhD-SNP; PolyPhen-1; PolyPhen-2; SIFT; SNAP; nsSNPAnalyzer; and PANTHER. The best performing tools (the first six listed) were combined into a consensus classifier Predict-SNP (*42*), resulting in significantly improved prediction performance, and at the same time returning results for all mutations (http://loschmidt.chemi.muni.cz/predictsnp/).

Induction of DNA Double-Strand Breaks

Exponentially growing primary or immortalized MEFs were plated at 10^5 in 2 ml of growth media into glass coverslip-based dishes 24 h prior to ^{137}Cs gamma-ray irradiation with a dose rate of 1.7 Gy/min, or into 2.5 μm Mylar®-based dishes 48 h prior to alpha-particle irradiation (^{238}Plutonium) at a dose rate of 0.5 Gy/s. After irradiation incubation at 37°C for the given repair time, DSBs were detected in MEFs by immunostaining.

Sister Chromatid Exchange

Exponentially growing immortalized MEFs were treated with 0.5 μg/ml MMC (Sigma-Aldrich), and incubated at 37°C for 2 h and the frequency of SCEs was evaluated in second-division metaphases, under a light microscope (100× objective; Olympus BX60, Preston, UK).

Multicolor Fluorescence In Situ Hybridization (mFISH)

Slides were stained using 21× Mouse mFISH kit (Metasystems, Altlussheim, Germany) according to the manufacturer's protocol. Metaphases were analyzed as previously described by Becker *et al.* (*43*). Karyotyping was performed with ISIS-software (Metasystems). Chromosome aberrations were recorded according to the mPAINT system (*44*).

RESULTS

The 129S2/SvHsd Mouse Strain Contains a Disease-Causing Ctip nsSNP that is Associated with Reduced Mouse Life Span and rAML

We identified 21 nsSNPs within the mouse *Ctip* gene using the Ensembl genome browser, and assessed for disease prediction using the Predict-SNP algorithm. Three of the mouse nsSNPs (P164L, Q418P and D762G) were predicted as disease-causing and one nsSNP (H338Y) was predicted as nearly disease-causing by the Predict-SNP algorithm (Supplementary Table S1A; http://dx.doi.org/10.

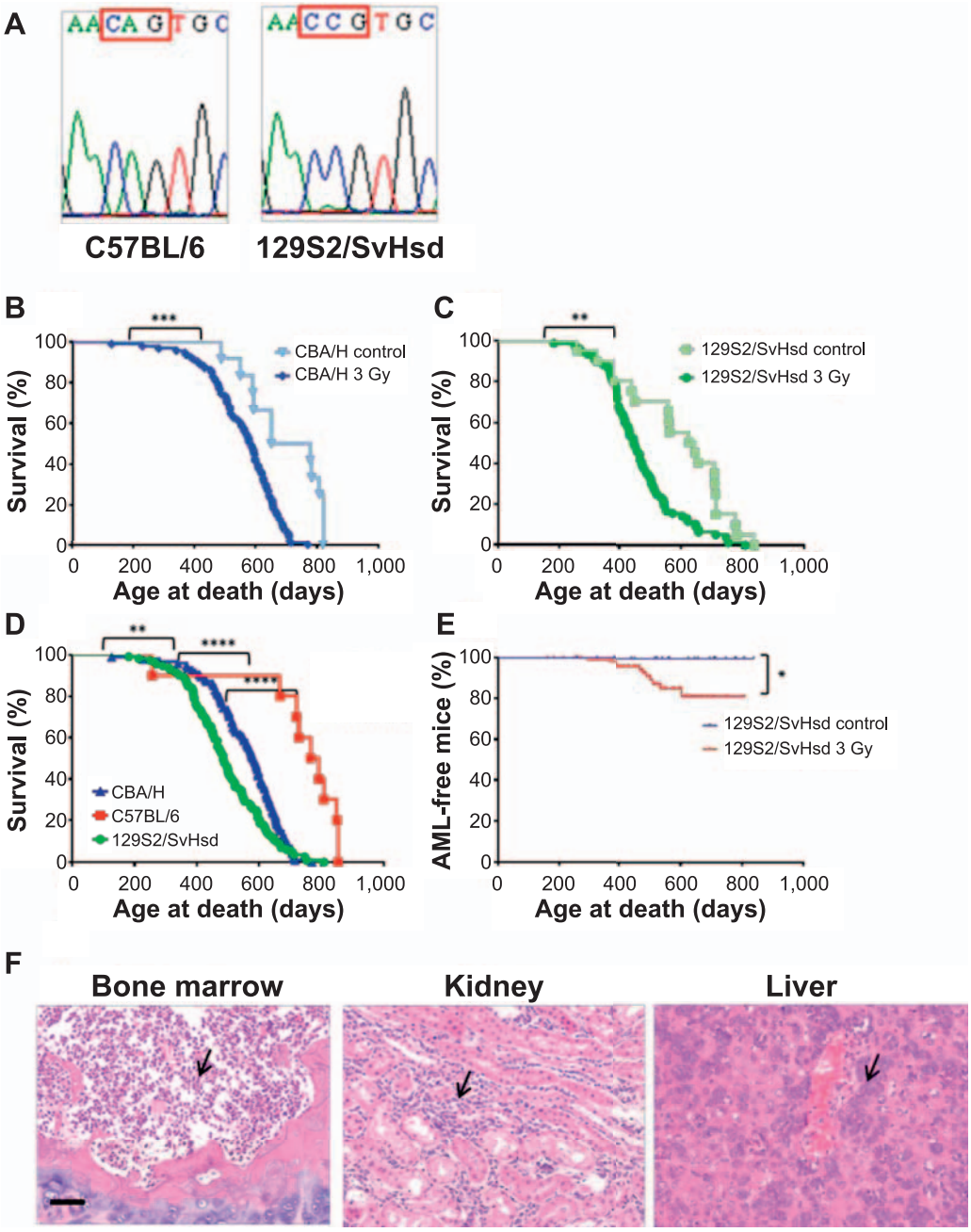

FIG. 1. Survival rate and AML development in 129S2/SvHsd mice after irradiation. Panel A: The DNA sequence from C57BL/6 and 129S2/SvHsd mice without or with a Q418P nsSNP in the *Ctip* gene, respectively. Substitution of adenine (A) with cytosine (C) results in amino acid change from glutamine (CAG) to proline (CCG). The survival percentage of controls versus 3 Gy X-ray irradiated mouse strains: CBA/H (panel B) and 129S2/SvHsd (panel C). The comparison of CBA/H, C57BL/6 and 129S2/SvHsd survival after exposure to 3 Gy of X rays (panel D). AML-free survival of radiation-exposed 129S2/SvHsd mice compared with control cohort (panel E). Example histopathology of irradiated 129S2/SvHsd mice; infiltration of bone marrow, kidney and liver by leukemic blasts (black arrows) (panel F). Statistical analysis: Kaplan-Meier analysis with a Mantel-Cox test, $*P < 0.05$; $**P < 0.01$; $****P < 0.0001$; scale bar: 100 μm.

1667/RR14495.1.S1). We screened for the presence of P164L, H338Y, Q418P and D762G nsSNPs using DNA from a large number of mouse strains (data not shown) and detected Q418P nsSNPs in the 129S2/SvHsd strain (Fig. 1A and Supplementary Table S1B). We further characterized the 129S2/SvHsd strain with *in vivo* and *in vitro* end points alongside the CBA/H and C57BL/6 strains, sensitive and resistant to rAML, respectively.

We observed that CBA/H and 129S2/SvHsd mice that were whole-body X-ray-irradiated with 3 Gy had shorter life spans compared to their respective nonirradiated controls (Fig. 1B and C). Our survival data indicate that of the three

mouse strains, 129S2/SvHsd mice are the most radiosensitive (Fig. 1D). However, when the mean life spans for the three irradiated mouse stains were normalized to the mean life spans of the corresponding controls, the 129S2/SvHsd strain showed a survival rate similar to the CBA/H-rAML sensitive strain postirradiation (Supplementary Table S2; http://dx.doi.org/10.1667/RR14495.1.S1).

We identified 11 (nine females, two males, 9.7%) mice with probable rAML within 113 (50 females, 63 males) irradiated 129S2/SvHsd mice (Fig. 1E). Radiation-induced AML was not observed in 26 sham-irradiated control mice (15 females, 11 males). Identification of potential AMLs was based on elevated white blood cell count, increased splenic weight, neutropenia and the presence of immature forms of white blood cells (leukemic blasts), when compared with nonirradiated 129S2/SvHsd controls (Supplementary Table S3A; http://dx.doi.org/10.1667/RR14495.1.S1). Confirmation was obtained by flow cytometry using a panel of cell surface markers (Supplementary Table S3C) and/or histological analysis (Fig. 1F). Seven cases analyzed by flow cytometry exhibited a greater percentage of leukemic blasts compared to control samples. Although 129S2/SvHsd mice exhibit lower incidence of rAML than CBA/H (*18*) (9.7 vs. 18%), the average latency for rAML development was shorter than the CBA/H strain, 370 and 450 days postirradiation, respectively.

We also observed tumors in different organs of 129S2/SvHsd mice: the Harderian glands (6.2% vs. 3.8% for controls), lung (4.4% vs. 0% for controls), testicles (6.2% vs. 0% for control males) and other organs (intestine, ovarian, pituitary gland) (13.3% vs. 7.7% for controls) (Supplementary Table S4). These data suggest that the nsSNP Q418P, found only in the 129S2/SvHsd mouse strain, may have affected life span, as well as influenced rAML induction and development of tumors in several organs after irradiation.

The Q418P nsSNP Impairs CTIP Function in HR

To assess whether the *Ctip* nsSNP alters efficiency of DNA repair and is affected by complexity of DNA damage, MEFs obtained from the three mouse strains, CBA/H, C57BL/6 and 129S2/SvHsd, were exposed to either low-linear energy transfer (LET) gamma radiation or high-LET alpha particles. DSB repair efficiency was determined using γ-H2AX and 53BP1 as markers of DSBs (*19*) (representative foci images Fig. 2C and D). With alpha particles, significant levels of residual DSBs persisted for at least 24 h postirradiation, in contrast to gamma rays where the majority of DSBs were repaired within 24 h. These observations corroborate the concept of increased complexity of DNA damage induced by high-LET alpha particles compared to low-LET gamma rays (*20*). We did not observe differences in the repair rate among the three MEF cell lines after 1 Gy gamma irradiation. However, after 1 Gy alpha irradiation, faster DSB repair was observed up to 6 h postirradiation in CBA/H and 129S2/SvHsd MEFs compared to C57BL/6 (Fig. 2A and B). These small differences observed may be related to the use of the NHEJ pathway in the repair of the simpler DSBs caused by low-LET radiation. Since γ-H2AX and 53BP1 are markers of DSBs repaired by both NHEJ and HR, we used Rad51 [which initiates strand invasion after DSB resection (*21*)] and RPA [which binds ssDNA after CTIP mediated resection (*12*)] as specific markers of HR to determine any differences in repair efficiency in the MEF cell lines.

To ascertain the optimal radiation dose needed to induce the level of Rad51 and RPA foci above background (untreated cells showed approximately 5% Rad51- or RPA-positive cells), a dose response was performed. The optimum dose of 10 Gy of gamma rays was chosen to assess whether any differences could be seen in the dynamics of formation and loss of Rad51 and RPA foci induced in CBA/H, C57BL/6 and 129S2/SvHsd cell lines.

We observed lower levels of recruitment of Rad51 and RPA to the damage sites, up to 8 h after 10 Gy irradiation in 129S2/SvHsd MEF cells compared to CBA/H and C57BL/6 MEF cells (Fig. 3A). Since CTIP is essential for recruitment of RPA to DSB ends during HR, we examined the levels of phosphorylated RPA32 (pRPA32) after exposure to 10 and 50 Gy of gamma radiation (Supplementary Fig. S1A; http://dx.doi.org/10.1667/RR14495.1.S1). Despite previous reports of increased pRPA32 after 50 Gy gamma irradiation (*22*), we did not detect pRPA32 at 1–24 h postirradiation with either dose. Since DSBs formed from stalled or collapsed replication forks are predominantly repaired by HR (*23*), we treated MEFs with 1 m*M* of HU [which impedes S-phase progression (*24*)] to address the possibility of Q418P affecting *Ctip*'s activity and role during HR when dealing with replication stress. We probed for RPA32 protein and observed its phosphorylated form at 6 and 24 h after HU treatment in both CBA/H and C57BL/6 MEFs, but crucially, not in 129S2/SvHsd MEFs (Supplementary Fig. S1B).

To verify these findings, we knocked down CTIP protein, and evaluated the level of RPA32 hyperphosphorylated at serine 4 and 8 (RPA32 pS4/S8) [reported to be the main site phosphorylated during DNA damage response (*24*)] 6 and 24 h after 1 m*M* HU treatment in control (shGFP) and CTIP (shCTIP) knockdown MEFs. The level of CTIP was significantly lower in CTIP knockdown (shCTIP) cells when compared to levels in control (shGFP) MEFs (Fig. 3D). HU treatment induced phosphorylation of RPA32 pS4/S8 at 6 and 24 h after HU treatment in CBA/H and C57BL/6 control MEFs (shGFP) but not in CTIP knockdown MEFs. In contrast, 129S2/SvHsd shGFP MEFs showed no RPA32 pS4/S8 at 6 h after HU treatment and only low levels of phosphorylation at 24 h. Similar to CBA/H and C57BL/6 cells with CTIP knockdown, 129S2/SvHsd shCTIP cells showed no RPA32 pS4/S8 at 6 and 24 h after HU treatment (Fig. 3D). We also evaluated the effect of CTIP knockdown on

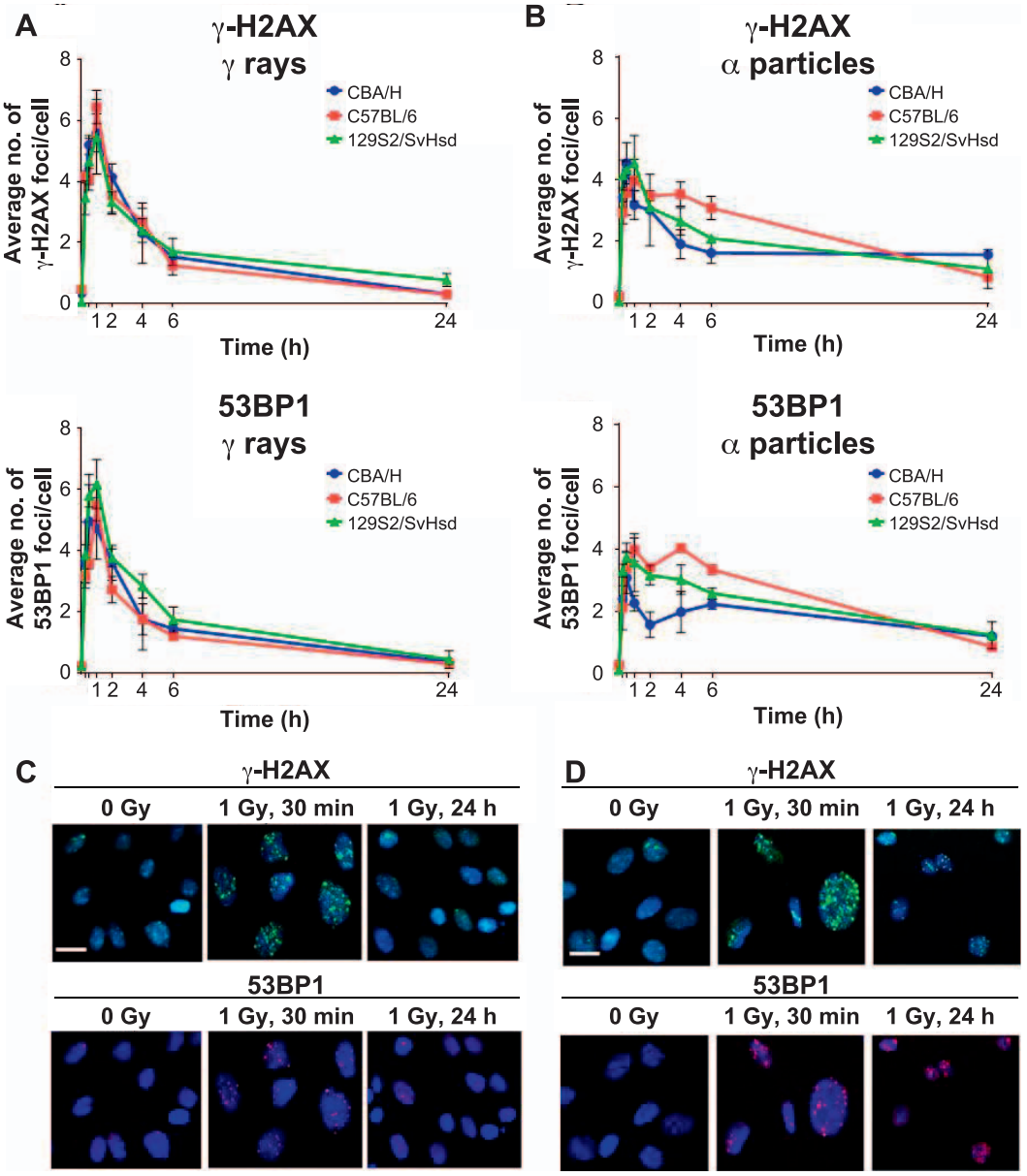

FIG. 2. DSB repair kinetics after gamma-ray and alpha-particle irradiation. Panels A and B: Formation of γ-H2AX and 53BP1 foci and loss in primary MEFs after exposure to 1 Gy of gamma rays (panel A, upper and lower panel) and 1 Gy alpha particles (panel B, upper and lower panel). Representative images of γ-H2AX and 53BP1 foci in C57BL/6 primary MEFs after exposure to 1 Gy of gamma rays (panel C) and 1 Gy of alpha particles (panel D) at stated time points. At least 50 cells per time point were counted. n = 3; ±SEM; scale bar: 100 μm.

Rad51 and RPA foci formation after irradiation. CTIP-depleted CBA/H and C57BL/6 MEFs (shCTIP) exhibited decreased Rad51- and RPA-positive cells (≥5 foci) at all time points studied, except at 24 h after 10 Gy gamma irradiation, when compared to controls (shGFP). In contrast, the numbers of Rad51- and RPA-positive cells in the CTIP-depleted 129S2/SvHsd MEFs were similar to those observed in 129S2/SvHsd cells expressing CTIP after 10 Gy gamma irradiation (Fig. 3A and B; representative foci images Fig. 3C). These observations with CTIP knockdown cells are consistent with those seen in the 129S2/SvHsd shGFP cells. This indicates that reduction of CTIP activity leads to impaired HR in 129S2/SvHsd MEFs, relative to CBA/H and C57BL/6 MEFs. Since ATR recruitment to replication-induced DSB ends is at least partially dependent on CTIP, ATR protein expression was also examined in MEFs after treatment with 1 m*M* HU for 6 h. 129S2/SvHsd MEFs exhibited much lower levels of ATR in comparison to CBA/H and C57BL/6 controls and HU-treated MEFs (Fig. 4A).

Since CTIP facilitates the recruitment of ATR to DSB ends, we propose that the lower levels of ATR protein seen

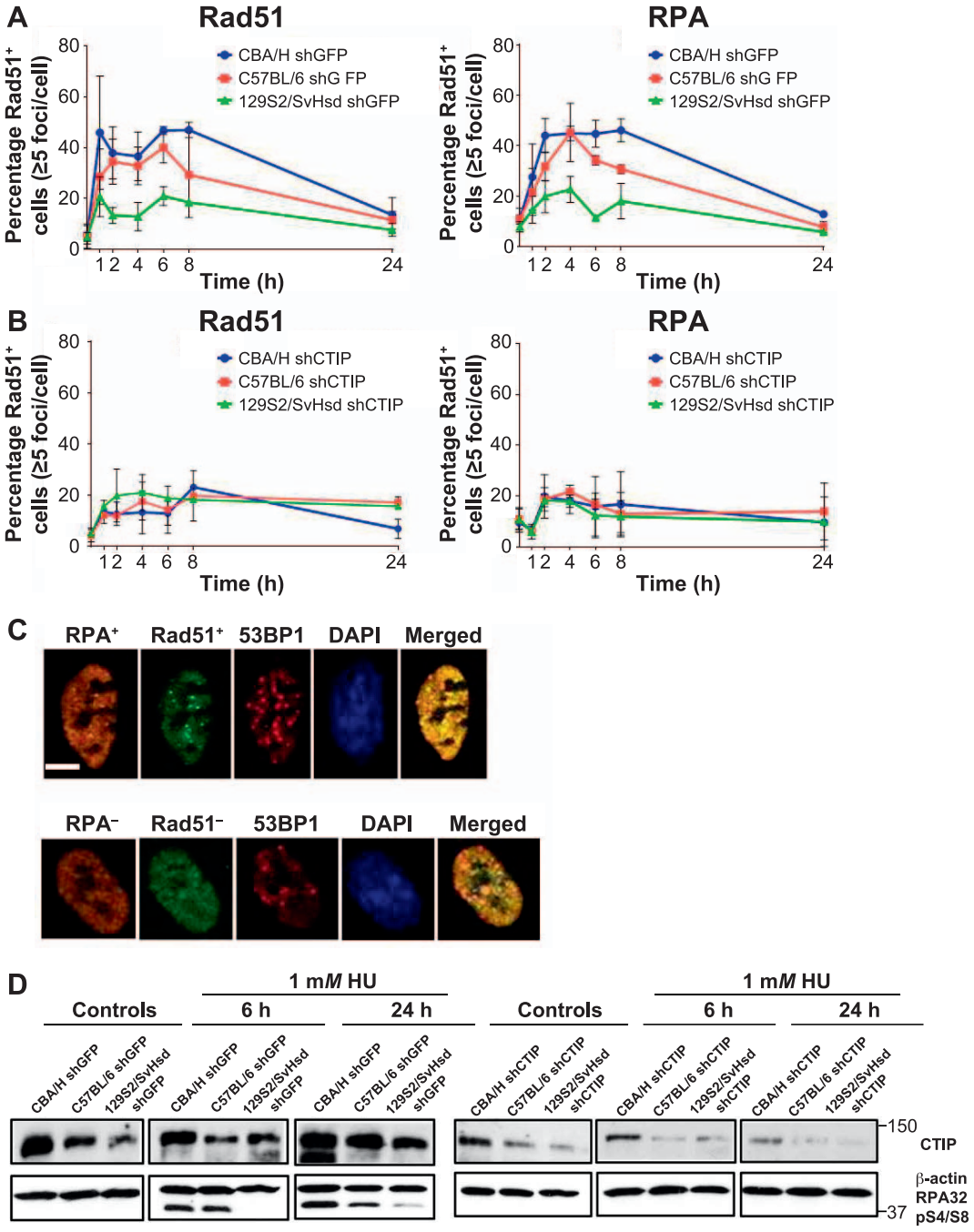

FIG. 3. The impairment of HR in 129S2/SvHsd cells, measured by the number of Rad51 and RPA foci. Panel A: The percentage of Rad51 (left panel) and RPA (right panel) positive cells in immortal MEF controls (shGFP) after exposure to 10 Gy of gamma radiation. Panel B: Corresponding CTIP knockdown cells (shCTIP) after exposure to 10 Gy of gamma radiation. Panel C: Representative images of Rad51$^+$ and RPA$^+$ immortal C57BL/6 cells $\geq$5 foci and Rad51$^-$ and RPA$^-$ cells $\leq$5 foci, as well as 53BP1 foci, 4 h after exposure to 10 Gy of gamma radiation. Panel D: The level of CTIP and RPA32 pS4/S8 expression in immortal MEF controls (shGFP, left panel) and CTIP knockdown cells (shCTIP, right panel), 6 and 24 h after 1 m*M* HU treatment. Beta-actin was used as a loading control. At least 50 cells per time point were counted. n = 3; ±SEM; scale bar: 10 μm.

in control as well as in the HU-treated 129S2/SvHsd cells, compared with the other two cells lines, are a result of impaired DSB resection as a consequence of reduced functionality of CTIP protein in these cells. This observation is consistent with the absence of pRPA32 in 129S2/SvHsd MEFs and confirms the reported role of active CTIP in recruitment of RPA and ATR to DNA damage sites.

To verify that the reduced activity of CTIP in 129S2/SvHsd MEFs is a consequence of the Q418P nsSNP, we overexpressed active CTIP in these cells, which restored the

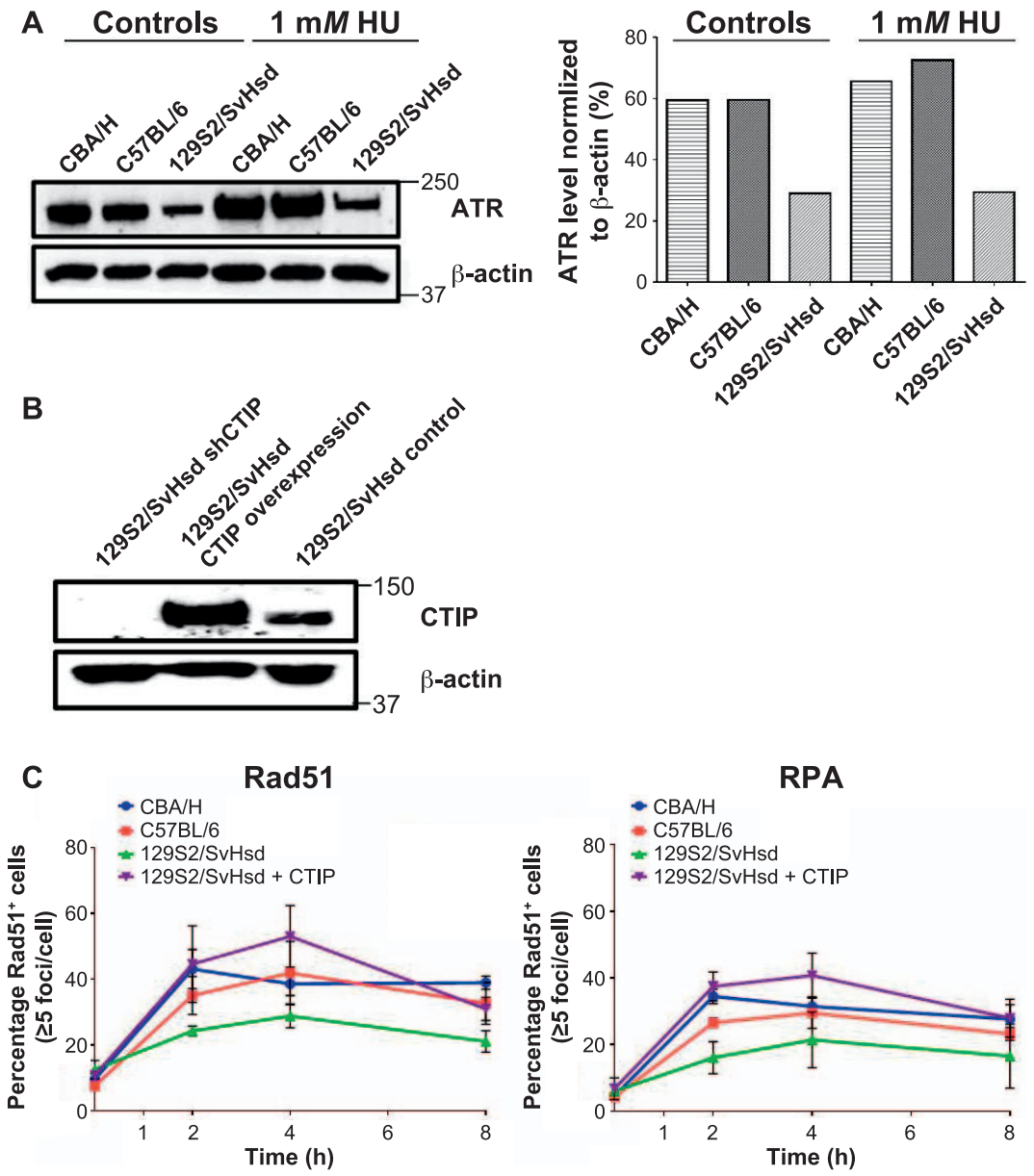

FIG. 4. Overexpression of active CTIP in 129S2/SvHsd cells rescues the phenotype. Panel A: The level of ATR protein in immortal MEFs (left panel); cells were treated with 1 m*M* HU for 6 h or remained untreated; the ATR protein level of each sample was normalized to its β-actin control (right panel). Panel B: Knockdown and overexpression of CTIP protein in 129S2/SvHsd cell line; β-actin was used as a loading control. C: The percentage of $Rad51^+$ (left panel) and RPA^+ (right panel) cells in immortal CBA/H, C57BL/6, 129S2/SvHsd and 129S2/SvHsd plus CTIP (129S2/SvHsd overexpressing CTIP) MEFs after exposure to 10 Gy of gamma radiation, n = 3; ± SEM.

number of radiation-induced Rad51- and RPA-positive cells (Fig. 4B and C).

We also examined the efficiency of HR using SCEs (*25*). Differences in the yield of SCEs among CBA/H, C57BL/6 and 129S2/SvHsd MEFs either treated with MMC [a DNA interstrand crosslinker and inducer of SCEs (*26*)] or exposed to alpha-particle radiation were investigated. The 129S2/SvHsd MEFs showed lower numbers of spontaneous and induced SCEs compared to the CBA/H and C57BL/6 MEFs (Fig. 5). This confirms that the Q418P nsSNP reduces CTIP's main function of DSB resection and leads to impaired HR.

The cell cycle distribution was very similar for C57BL/6 and 129S2/SvHsd, whereas CBA/H MEFs exhibited a slightly lower S-phase population (Supplementary Fig. S2; http://dx.doi.org/10.1667/RR14495.1.S1). This indicates that the lower percentage of Rad51- and RPA-positive cells observed in 129S2/SvHsd MEFs is not due to significant differences in the S-phase population among the cell lines.

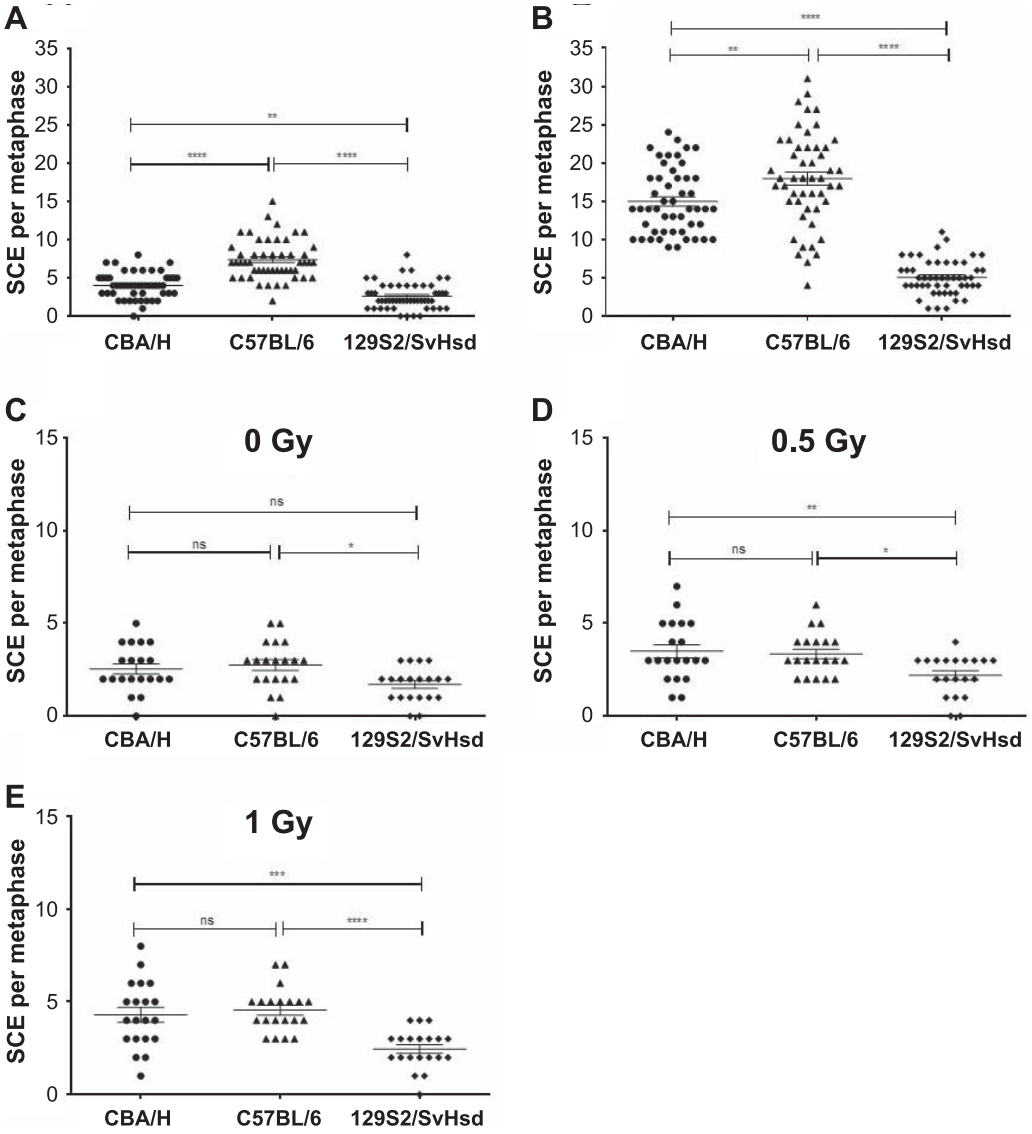

FIG. 5. Low level of HR in 129S2/SvHsd cells, determined by reduced number of SCEs. Comparison of spontaneous (panel A), and MMC-induced (panel B) SCEs in immortal MEFs; 50 metaphase spreads were scored per cell line. Comparison of the frequency of spontaneous 0 (panel C), 0.5 (panel D) and 1 Gy (panel E) alpha-particle-induced SCEs in MEFs; 20 metaphase spreads were scored per cell line, ± SEM; Statistical analysis: one-way analysis of variances (ANOVAs), ns = nonsignificant, $*P > 0.05$, $**P < 0.01$, $***P < 0.001$, $****P < 0.0001$.

No differences were observed in cell survival among the CBA/H, C57BL/6 and 129S2/SvHsd MEFs after γ irradiation (Supplementary Fig. S3), probably due to the use of NHEJ or SSA in 129S2/SvHsd, as alternatives to impaired HR.

The impairment of *Ctip* has been associated with genomic instability, including chromosome translocations. In their published study, Zhang and Jasin (*27*) reported on a model in which CTIP-mediated alt-NHEJ plays a major role in translocation formation. They observed a decrease in chromosomal translocation frequency in mouse cells with CTIP knockout, and suggested that targeting CTIP has therapeutic potential to reduce translocations. Based on those observations, we anticipated that impairment of *Ctip* via the Q418P nsSNP would potentially affect the rate of translocations *in vivo*. Therefore, we performed a chromosomal analysis on splenocytes 48 h after 2 Gy X irradiation *in vivo* (Fig. 6). We observed very low numbers of *de novo* aberrations (≤0.03–0.06 aberrations/cell) in splenocytes of nonirradiated mice. No differences were seen in terms of scored translocations, dicentrics and Robertsonian translocations among the three cell lines: CBA/H, C57BL/6 and 129S2/SvHsd. However, exposure to X rays did result in a pronounced increase in the number of aberrations per cell in all strains. Additionally, we observed a significant increase in exchanges involving three or more breaks in two or more chromosomes (complex aberrations) in 129S2/SvHsd compared to

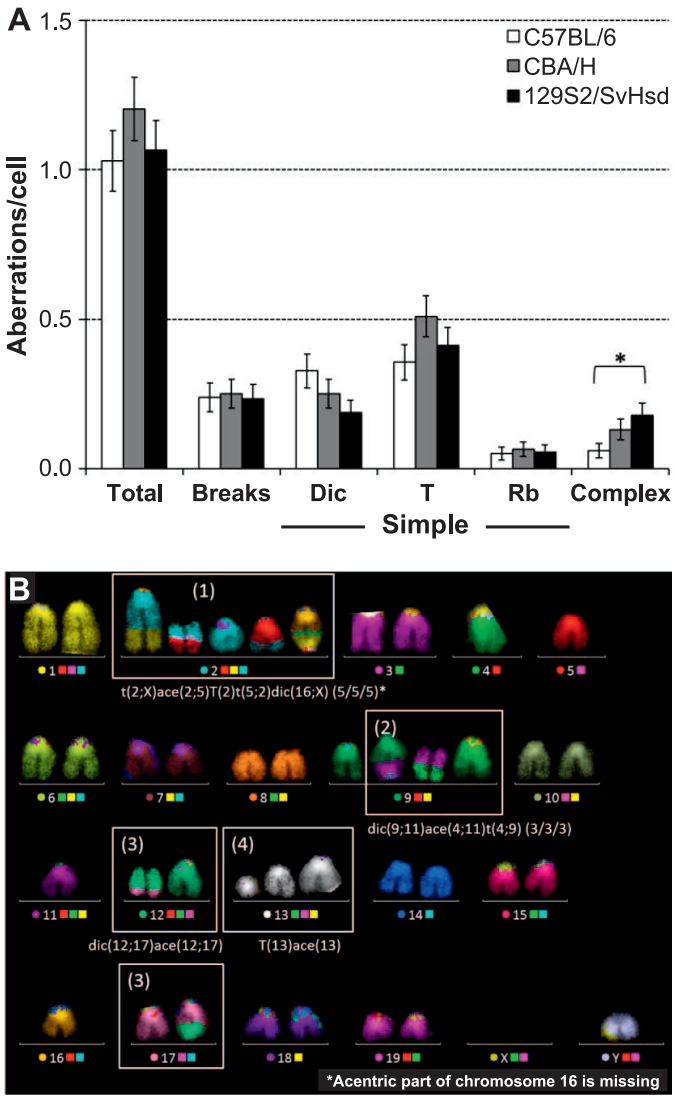

FIG. 6. Radiation-induced increase in complex aberrations in splenocytes from 129/SvHsd mice. Panel A: Chromosomal aberrations analyzed 48 h after exposure to 2 Gy of X rays in at least 100 metaphases using mFISH. Aberrations observed: breaks, dicentrics (Dic), translocations (T), Robertsonian translocations (Rb) and complex exchanges (involving three or more breaks in two or more chromosomes); controls: 0.03–0.06 aberrations/cell; ±SEM; Statistical analysis: Chi square test, $*P < 0.05$, all the other comparisons were nonsignificant ($P > 0.3$). Panel B: Example of chromosomal aberrations found in 129S2/SvHsd: forms (1) and (2) displaying two complex aberrations resulting from 5 breaks in 5 chromosomes and 3 breaks in 3 chromosomes, respectively; forms (3) and (4) show a dicentric and truncated chromosome, respectively.

C57BL/6 (Fig. 6). These data suggest that the defect in HR in 129S2/SvHsd cells due to the presence of the Q418P nsSNP impairs the correct repair of complex DSBs, leading to complex aberrations. The differences between the observations of Zhang and Jasin and our data may reflect differences in experimental setup. Zhang and Jasin performed *in vitro* experiments with CTIP knockout cells, whereas we performed *in vivo* experiments in cells harboring a Q418P nsSNP within the *Ctip* gene.

DISCUSSION

In this study, we have characterized the 129S2/SvHsd mouse strain, which carries an *in silico* identified, potentially disease-causing Q418P nsSNP within the *Ctip* gene (Fig. 1A and Supplementary Table S1; http://dx.doi.org/10.1667/RR14495.1.S1). Our experiments have shown that Q418P strongly influences CTIP function in the repair of DSBs by HR and it could be linked to radiation-induced leukemogenesis.

The 129 strain has a long life span under conventional conditions, with low overall tumor incidence. While the 129S2/SvHsd substrain also has a low incidence of spontaneous tumors, its level of radiosensitivity leading to early-onset tumors, including rAML, has been unknown (*28*). Our *in vivo* experiments demonstrated similar mean life spans for 129S2/SvHsd and CBA/H after 3 Gy X irradiation, when normalized to controls (82% and 75%, respectively) (Supplementary Table S2, http://dx.doi.org/10.1667/RR14495.1.S1), indicating that 129S2/SvHsd is a radiosensitive strain. Radiosensitivity was measured as mean life span after one 3 Gy dose, and not as a mean life span after daily whole-body exposure to 1 Gy of X-ray radiation, as previously reported by Roderick (*29*), where the 129 strain was radioresistant. Additionally, Roderick's experiments were performed with a different substrain of 129 (129/J), which may not carry the Q418P nsSNP within the *Ctip* gene.

General life span shortening after irradiation was partly associated with an increase in cancer rate. Testicular and lung tumors were found in the irradiated group but not in the controls (Supplementary Table S4; http://dx.doi.org/10.1667/RR14495.1.S1). There were seven testicular tumors and five lung tumors in the irradiated group, with three lung cases confirmed as bronchioalveolar adenoma by histopathology. Since lungs are prone to radiation-induced cancer (*30*), it is tempting to suggest that a link exists, however, further experiments are required to confirm this finding. In our previously published work, we predicted a strong link between CTIP and rAML (*7*), and in this study, we identified and characterized a 129 substrain that may be predisposed to rAML, since 9.7% of the irradiated 129S2/SvHsd mice were diagnosed with rAML (Fig. 1E). The number of rAML cases was lower than that in CBA/H mice (18%), a strain well known for developing rAML (*18*). Nevertheless, this is a relatively high rate, since mice rarely develop AML *de novo*.

In the CBA mouse model of rAML, chromosome 2 deletions are a consistent feature (*31*), however, this deletion was found only in one out of the 11 cases, analyzed by comparative genome hybridization (Supplementary Fig. S4; http://dx.doi.org/10.1667/RR14495.1.S1), suggesting that the molecular mechanisms of leukemogenesis are different in 129S2/SvHsd and possibly associated with a reduction in CTIP efficiency. Taken together, the experimental data demonstrate that this specific mouse

substrain may be predisposed to rAML and that Q418P nsSNP, found only in the 129S2/SvHsd strain, may influence the life span as well as early onset of radiation-induced AML and other tumors.

DSBs are potentially lethal lesions that can lead to chromosomal rearrangements if unrepaired or misrepaired. Radiation-induced AML may be a direct consequence of the significantly increased level of complex chromosomal aberrations found in 129S2/SvHsd splenocytes irradiated *in vivo* (Fig. 6). Moreover, we observed lower levels of recruitment of HR markers (Rad51 and RPA) to radiation-induced damage sites in 129S2/SvHsd compared to CBA/H and C57BL/6 MEFs (Fig. 3A). Similarly, phosphorylation of RPA32, induced by HU treatment, was observed in CBA/H and C57BL/6 cells but not in 129S2/SvHsd MEFs (Fig. 3D). In addition, ATR expression was significantly lower in 129S2/SvHsd, independent of HU treatment, compared to the other two MEF cell lines (Fig. 4A). Knockdown of CTIP in the three MEF cell lines indicates that DSB resection is impaired due to reduced CTIP activity (Fig. 3B and C). These findings are consistent with previously published data, showing that the activation of RPA (*24*), Rad51 (*21*) and ATR (*32*), the key proteins involved in HR of DSBs, is CTIP-dependent (*12*). Overexpression of active CTIP in 129S2/SvHsd cells restored the number of Rad51- and RPA-positive cells postirradiation (Fig. 4C), indicating that reduced CTIP activity in 129S2/SvHsd cells is a consequence of the Q418P nsSNP.

We also observed lower numbers of spontaneous, MMC and alpha-particle-induced SCEs in 129S2/SvHsd MEFs, compared to CBA/H and C57BL/6 cell lines (Fig. 5). This finding is consistent with published studies showing that cells defective in HR (e.g., cells depleted of BRCA2 or Rad51) exhibit reduced numbers of SCEs (*25, 33*). Therefore, we propose that the Q418P nsSNP within *Ctip* of 129S2/SvHsd MEFs has a strong influence on the efficiency of CTIP function in HR repair of DSBs.

CTIP plays a major role in HR, but it is also involved in alt-NHEJ, which is error prone and contributes to chromosomal translocations and telomere fusions (*34*). Our data provides, to our knowledge, the first evidence of the role of CTIP in chromosomal aberrations formation *in vivo*, after X-ray irradiation. These findings (i.e., comparable levels of translocations among three mouse strains, but an increase in complex aberrations in 129S2/SvHsd stain) provide valuable information about CTIP's function.

Mutations in NHEJ and HR genes have been linked to both cancer and immune deficiencies, and genes such as *Ctip* are expected to have low tolerance for mutations. Mikkelsen *et al*. analyzed the molecular evolution of NHEJ genes in primates and humans (*35*) and found support for positive selection in five NHEJ genes, among which was *Ctip*. Mutations in the human *CTIP* gene have been described in the literature, including mutations in a conserved CDK site (T847) that reduced the level of alt-NHEJ and HR, implicating CTIP as a critical target of CDKs to promote HR and short-range end resection to activate alt-NHEJ (*36*).

The identification of *Ctip* as a potential susceptibility gene for rAML underscores the important role of the DNA repair gene family in radiation-induced tumorigenesis. Mutations such as microsatellite length variation or nsSNPs have been previously detected in DNA damage response genes. Microsatellite instability dependent mutations in the *CTIP* and *MRE11* genes have been identified in myeloid malignancies (*37*). NsSNPs have been found in the Nijmegen breakage syndrome 1 (*NBS1*) gene of patients diagnosed with hepatocellular carcinoma, intrahepatic cholangiocarcinoma (*38*), and Seckel and Jawad syndrome, characterized by the presence of nsSNPs leading to expression of a C-terminally truncated protein (*39*). Cells derived from Seckel patients are impaired in ATR signaling and in G_2/M cell cycle checkpoint arrest when exposed to ultraviolet (UV) light or replication-stalling agents such as HU (*40*). This is in agreement with our data showing lower levels of ATR protein in 129/SvHsd MEFs compared to CBA/H and C57BL/6. Gaymes *et al*. (*37*) reported that genomic instability dependent mutations in the *Ctip* gene partially impaired CTIP activity during HR. Furthermore, they observed a 50% reduction in *Ctip* expression, leading to HR inhibition, in leukemic blast cells obtained from patients diagnosed with AML. Heterozygous expression of *CTIP* in an AML patient was associated with normal cell cycle kinetics and the *CTIP* mutation led to a DNA repair anomaly only detected using poly (ADP-Ribose) polymerase inhibitors. To compare with our study, the cell cycle kinetics are also normal in 129S2/SvHsd, and we suggest that Q418P partially impairs CTIP activity that can only be detected after HR-dependent repair of DNA damage. Mice develop normally and are not prone to cancer development, suggesting a higher CTIP activity than in *CTIP* heterozygote mice where haploid insufficiency leads to tumorigenesis, predominantly lymphoma.

While the Q418 nsSNP has not been reported in the human CTIP gene to date, there are many nsSNPs present in this gene (approximately 100) and nearby nsSNPs, at positions 402, 412, 414 and 425, reported to lead to missense mutations in humans. It would be of great interest to search for the presence of these nsSNPs in the DNA of patients diagnosed with AML, or more specifically those who develop therapy-related AML (t-AML), especially radiotherapy-related AML.

In conclusion, this study has shown that the mouse Q418P nsSNP impairs CTIP activity in HR after gamma-ray- and alpha-particle-induced DNA damage *in vitro*, and it is associated with a high frequency of complex chromosomal aberrations and most probably tumorigenesis (including rAML) after X-ray exposure *in vivo*. Such studies help to improve the understanding of genetic risk factors and predisposition to radiation-induced carcinogenesis.

SUPPLEMENTARY INFORMATION

Supplementary data are available at http://dx.doi.org/10.1667/RR14495.1.S1. Supplementary figures S1–S4 and Tables S1–S4.

ACKNOWLEDGMENTS

We thank, Dr. Madalena Tarsounas, Oxford Institute of Radiation Biology, Oxford, UK for transfection constructs, reagents for immortalization of MEFs and CTIP knockdown, and pRPA32 (S4/S8) antibody, Dr. Richard Baer, Columbia University, New York for CTIP antibody, Dr. Andre Nussenzweig, National Cancer Institute, Bethesda, MD, for Retro-Super plasmid with shRNA for CTIP knockdown, Dr. James Thompson, Dr. Mark Hill and Luke Bird for gamma and alpha irradiation, Mick Woodcock for help with FACS analysis. We also thank Joanna Zyla, Silesian University of Technology, Gliwice, Poland, for help with bioinformatical analysis. This work was supported by the National Institute for Health Research Centre in Public Health Protection, the Medical Research Council (MC PC 12001) and by the European Union FP7 DoReMi Network of Excellence (grant no. 249689). The authors declare no competing financial interests.

Received: April 22, 2016; accepted: August 2, 2016; published online: November 21, 2016

REFERENCES

1. Rahman N. Realizing the promise of cancer predisposition genes. Nature 2014; 505:302–8.
2. Figueroa JD, Ye Y, Siddiq A, Garcia-Closas M, Chatterjee N, Prokunina-Olsson L, et al. Genome-wide association study identifies multiple loci associated with bladder cancer risk. Hum Mol Genet 2014; 23 5:1387–98.
3. Cai Q, Zhang B, Sung H, Low SK, Kweon SS, Lu W, et al. Genome-wide association analysis in East Asians identifies breast cancer susceptibility loci at 1q32.1, 5q14.3 and 15q26.1. Nat Genet 2014; 46:886–90.
4. Speedy HE, Di Bernardo MC, Sava GP, Dyer MJ, Holroyd A, Wang Y, et al. A genome-wide association study identifies multiple susceptibility loci for chronic lymphocytic leukemia. Nat Genet 2014; 46:56–60.
5. Ellinghaus E, Stanulla M, Richter G, Ellinghaus D, te Kronnie G, Cario G, et al. Identification of germline susceptibility loci in ETV6-RUNX1-rearranged childhood acute lymphoblastic leukemia. Leukemia 2012; 26:902–9.
6. Knight JA, Skol AD, Shinde A, Hastings D, Walgren RA, Shao J, et al. Genome-wide association study to identify novel loci associated with therapy-related myeloid leukemia susceptibility. Blood 2009; 113:5575–82.
7. Darakhshan F, Badie C, Moody J, Coster M, Finnon R, Finnon P, et al. Evidence for complex multigenic inheritance of radiation AML susceptibility in mice revealed using a surrogate phenotypic assay. Carcinogenesis 2006; 27:311–8.
8. Schaeper U, Subramanian T, Lim L, Boyd JM, Chinnadurai G. Interaction between a cellular protein that binds to the C-terminal region of adenovirus E1A (CtBP) and a novel cellular protein is disrupted by E1A through a conserved PLDLS motif. J Biol Chem 1998; 273:8549–52.
9. Yu X, Baer R. Nuclear localization and cell cycle-specific expression of CtIP, a protein that associates with the BRCA1 tumor suppressor. J Biol Chem 2000; 275:18541–9.
10. Parisi T, Bronson RT, Lees JA. Inactivation of the retinoblastoma gene yields a mouse model of malignant colorectal cancer. Oncogene 2015; 34:5890–9.
11. Yun MH, Hiom K. CtIP-BRCA1 modulates the choice of DNA double-strand-break repair pathway throughout the cell cycle. Nature 2009; 459:460–3.
12. Sartori AA, Lukas C, Coates J, Mistrik M, Fu S, Bartek J, et al. Human CtIP promotes DNA end resection. Nature 2007; 450:509–14.
13. Bennardo N, Cheng A, Huang N, Stark JM. Alternative-NHEJ is a mechanistically distinct pathway of mammalian chromosome break repair. PLoS Genet 2008; 4:e1000110.
14. Chen PL, Liu F, Cai S, Lin X, Li A, Chen Y, et al. Inactivation of CtIP leads to early embryonic lethality mediated by G1 restraint and to tumorigenesis by haploid insufficiency. Mol Cell Biol 2005; 25:3535–42.
15. Peterson SE, Li Y, Wu-Baer F, Chait BT, Baer R, Yan H, et al. Activation of DSB processing requires phosphorylation of CtIP by ATR. Mol Cell 2013; 49:657–67.
16. Wang H, Shi LZ, Wong CC, Han X, Hwang PY, Truong LN, et al. The interaction of CtIP and Nbs1 connects CDK and ATM to regulate HR-mediated double-strand break repair. PLoS Genet 2013; 9:e1003277.
17. Liu S, Opiyo SO, Manthey K, Glanzer JG, Ashley AK, Amerin C, et al. Distinct roles for DNA-PK, ATM and ATR in RPA phosphorylation and checkpoint activation in response to replication stress. Nucleic Acids Res 2012; 40:10780–94.
18. Olme CH, Finnon R, Brown N, Kabacik S, Bouffler SD, Badie C. Live cell detection of chromosome 2 deletion and Sfpi1/PU1 loss in radiation-induced mouse acute myeloid leukaemia. Leuk Res 2013; 37:1374–82.
19. Yajima H, Fujisawa H, Nakajima NI, Hirakawa H, Jeggo PA, Okayasu R, et al. The complexity of DNA double strand breaks is a critical factor enhancing end-resection. DNA Repair (Amst) 2013; 12:936–46.
20. Jenner TJ, deLara CM, O'Neill P, Stevens DL. Induction and rejoining of DNA double-strand breaks in V79-4 mammalian cells following gamma- and alpha-irradiation. Int J Radiat Biol 1993; 64:265–73.
21. Simandlova J, Zagelbaum J, Payne MJ, Chu WK, Shevelev I, Hanada K, et al. FBH1 disrupts RAD51 filaments in vitro and modulates homologous recombination in mammalian cells. J Biol Chem 2013; 288:34168–80.
22. Cheng X, Cheong N, Wang Y, Iliakis G. Ionizing radiation-induced phosphorylation of RPA p34 is deficient in ataxia telangiectasia and reduced in aged normal fibroblasts. Radiother Oncol 1996; 39:43–52.
23. Shi W, Feng Z, Zhang J, Gonzalez-Suarez I, Vanderwaal RP, Wu X, et al. The role of RPA2 phosphorylation in homologous recombination in response to replication arrest. Carcinogenesis 2010; 31:994–1002.
24. Liaw H, Lee D, Myung K. DNA-PK-dependent RPA2 hyperphosphorylation facilitates DNA repair and suppresses sister chromatid exchange. PLoS One 2011; 6:e21424.
25. Conrad S, Kunzel J, Lobrich M. Sister chromatid exchanges occur in G2-irradiated cells. Cell Cycle 2011; 10:222–8.
26. Wojcik A, Stoilov L, Szumiel I, Legerski R, Obe G. Rad51C-deficient CL-V4B cells exhibit normal levels of mitomycin C-induced SCEs but reduced levels of UVC-induced SCEs. Biochem Biophys Res Commun 2005; 326:805–10.
27. Zhang Y, Jasin M. An essential role for CtIP in chromosomal translocation formation through an alternative end-joining pathway. Nat Struct Mol Biol 2011; 18:80–4.
28. Storer JB. Longevity and gross pathology at death in 22 inbred mouse strains. J Gerontol 1966; 21:404–9.
29. Roderick TH. The response of twenty-seven inbred strains of mice to daily doses of whole-body X-irradiation. Radiat Res 1963; 20:631–9.
30. Fabrikant JI. Radon and lung cancer: the BEIR IV Report. Health Phys 1990; 59:89–97.
31. Peng Y, Brown N, Finnon R, Warner CL, Liu X, Genik PC, et al.

Radiation leukemogenesis in mice: loss of PU.1 on chromosome 2 in CBA and C57BL/6 mice after irradiation with 1 GeV/nucleon 56Fe ions, X rays or gamma rays. Part I. Experimental observations. Radiat Res 2009; 171:474–83.

32. Sancar A, Lindsey-Boltz LA, Unsal-Kacmaz K, Linn S. Molecular mechanisms of mammalian DNA repair and the DNA damage checkpoints. Annu Rev Biochem 2004; 73:39–85.

33. Xu H, Balakrishnan K, Malaterre J, Beasley M, Yan Y, Essers J, et al. Rad21-cohesin haploinsufficiency impedes DNA repair and enhances gastrointestinal radiosensitivity in mice. PLoS One 2010; 5:e12112.

34. Simsek D, Jasin M. Alternative end-joining is suppressed by the canonical NHEJ component Xrcc4-ligase IV during chromosomal translocation formation. Nat Struct Mol Biol 2010; 17:410–6.

35. Mikkelsen TS, Hillier LW, Eichler EE, Zody MC, Jaffe DB, Yang S-P, et al. Initial sequence of the chimpanzee genome and comparison with the human genome. Nature 2005; 437:69–87.

36. Huertas P, Jackson SP. Human CtIP mediates cell cycle control of DNA end resection and double strand break repair. J Biol Chem 2009; 284:9558–65.

37. Gaymes TJ, Mohamedali AM, Patterson M, Matto N, Smith A, Kulasekararaj A, et al. Microsatellite instability induced mutations in DNA repair genes CtIP and MRE11 confer hypersensitivity to poly (ADP-ribose) polymerase inhibitors in myeloid malignancies. Haematologica 2013; 98:1397–406.

38. Wang Y, Hong Y, Li M, Long J, Zhao YP, Zhang JX, et al. Mutation Inactivation of Nijmegen Breakage Syndrome Gene (NBS1) in Hepatocellular Carcinoma and Intrahepatic Cholangiocarcinoma. PLoS One 2013; 8:e82426.

39. Qvist P, Huertas P, Jimeno S, Nyegaard M, Hassan MJ, Jackson SP, et al. CtIP mutations cause Seckel and Jawad Syndromes. PLoS Genet 2011; 7:e1002310.

40. Alderton GK, Joenje H, Varon R, Borglum AD, Jeggo PA, O'Driscoll M. Seckel syndrome exhibits cellular features demonstrating defects in the ATR-signalling pathway. Hum Mol Genet 2004; 13:3127–38.

41. Kogan SC, Ward JM, Anver MR, Berman JJ, Brayton C, Cardiff RD, et al. Bethesda proposals for classification of nonlymphoid hematopoietic neoplasms in mice. Blood 2002; 100:238–45.

42. Bendl J, Stourac J, Salanda O, Pavelka A, Wieben ED, Zendulka J, et al. PredictSNP: robust and accurate consensus classifier for prediction of disease-related mutations. PLoS Comput Biol 2014; 10:e1003440.

43. Becker D, Elsasser T, Tonn T, Seifried E, Durante M, Ritter S, et al. Response of human hematopoietic stem and progenitor cells to energetic carbon ions. Int J Radiat Biol 2009; 85:1051–9.

44. Cornforth MN. Analyzing radiation-induced complex chromosome rearrangements by combinatorial painting. Radiat Res 2001; 155:643–59.